

ELECTRON COOLING RATES CHARACTERIZATION AT FERMILAB'S RECYCLER*

L.R. Prost[#], A. Shemyakin, FNAL, Batavia, IL 60510, U.S.A.

Abstract

A 0.1 A, 4.3 MeV DC electron beam is routinely used to cool 8 GeV antiprotons in Fermilab's Recycler storage ring [1]. The primary function of the electron cooler is to increase the longitudinal phase-space density of the antiprotons for storing and preparing high-density bunches for injection into the Tevatron. The longitudinal cooling rate is found to significantly depend on the transverse emittance of the antiproton beam. The paper presents the measured rates and compares them with calculations based on drag force data.

INTRODUCTION

The most important characteristic of the Recycler cooler's efficiency is the longitudinal cooling rate. This rate can be calculated in a non-magnetized model, assuming that electron beam parameters are known. On the other hand, an estimation of the rate can be made in a semi-empirical way, using the results of the drag force measurements. After explaining these approaches, we describe the cooling rate measurements and discuss the results.

LONGITUDINAL COOLING RATE CALCULATIONS

The longitudinal cooling rate in the lab frame can be expressed as a time derivative of the r.m.s. antiproton momentum width $\delta p = \gamma \sigma_{pz} M_p$, where $\gamma = 1/\sqrt{1-\beta^2}$, σ_{pz} is the r.m.s. spread of the longitudinal velocities of antiprotons in the beam frame, and M_p is the proton mass. Then, for a coasting antiproton beam, the longitudinal cooling rate relates to the longitudinal friction force F_z as

$$\frac{d}{dt} \left(\frac{\delta p^2}{2} \right) = \gamma M_p \int F_z(\vec{V}_p, \vec{r}_p) f_p(\vec{V}_p, \vec{r}_p) V_{pz} d\vec{V}_p d\vec{r}_p, \quad (1)$$

where f_p is the antiprotons velocity distribution and V_{pz} , the longitudinal component of the antiprotons velocity in the beam frame. \vec{V}_p and \vec{r}_p indicate the antiprotons velocity and position dependence of the friction force and velocity distribution.

Assuming a non-magnetized model for the friction force [2] with a constant Coulomb logarithm and constant electron beam properties across the area occupied by the antiproton beam, one can express the friction force as a single integral, called Binney's formula in Ref. [3], and drop the radial dependence in Eq. (1). As shown in Ref. [4], with the additional assumptions that f_p is Gaussian, and that the transverse velocity distribution is axially symmetrical for both electrons and antiprotons, all integrals can be carried out analytically so that Eq. (1) reduces to

$$\frac{d}{dt} \delta p = -\sqrt{2} \frac{4\pi m_e r_e^2 c^4 n_{eb} \eta L_c \sigma_{pz}}{\pi \sqrt{\sigma_{ez}^2 + \sigma_{pz}^2} (\sigma_{ex}^2 + \sigma_{px}^2)} \cdot f_{long}(\alpha), \quad (2)$$

$$f_{long}(\alpha) = \frac{1 - \sqrt{\frac{\alpha}{1-\alpha}} \cdot \arccos(\sqrt{\alpha})}{1-\alpha}, \quad \alpha = \frac{\sigma_{ez}^2 + \sigma_{pz}^2}{\sigma_{ex}^2 + \sigma_{px}^2}.$$

where σ_{ex} and σ_{ez} are the electron transverse and longitudinal rms velocity spreads in the beam frame, σ_{px} is the antiproton transverse rms velocity spread in the beam frame, m_e is the mass of the electron, r_e is the electron classical radius, n_{eb} is the electron beam density in the beam frame, η is the fraction of the ring occupied by the electron cooler and L_c is the Coulomb logarithm.

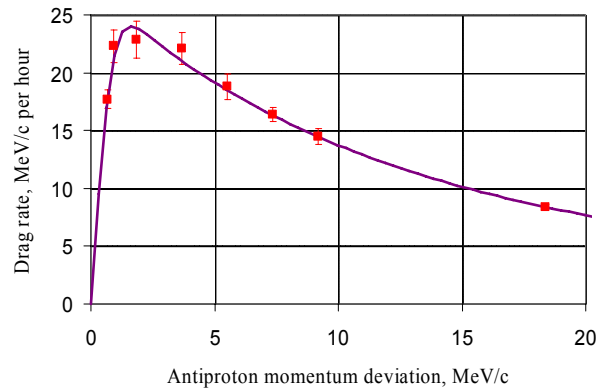


Figure 1: Drag rate as a function of the antiproton momentum deviation. $I_b = 0.1$ A, electron beam is on axis. The solid line is a fit by Eq. (3). $N_p = 3.5 \times 10^{10}$; the transverse emittance is $< 1 \pi$ mm mrad (normalized, 95%).

Eq. (2) gives the expected longitudinal cooling rate as a function of the electron beam main parameters such as its current density, its rms value of the electron angle spread and its rms energy spread. However, we found noticeable inconsistencies between independently measured electron beam parameters and those resulting from fits to drag force measurements [5]. On the other hand, if there is no correlation between the longitudinal and transverse antiproton distributions, Eq. (2) can be interpreted as a result of the integration of the function that best fits the measured drag rate data, over the antiproton distribution. Figure 1 shows the drag rates measured at various momentum deviations $p \equiv P - P_0 = \gamma M_p V_{pz}$ [1] and the fitting function derived from the non-magnetized model in a form optimized for the fitting algorithm [4]:

$$F_z(p) = -F_0 \cdot \int_0^{p/p_1} \frac{e^{-u^2} u^2}{u^2 + \left(\frac{p}{p_2}\right)^2} du, \quad (3)$$

where the fitting parameters p_1 , p_2 and F_0 relate to the electron beam parameters as follows:

$$\begin{aligned} p_1 &= \sqrt{2} \gamma M_p \sigma_{ez} , \\ p_2 &= \sqrt{2} \gamma M_p \sqrt{\sigma_{ex}^2 + \sigma_{px}^2 - \sigma_{ez}^2} , \\ F_0 &= \frac{\gamma n_{eb}}{\sigma_{ex}^2 + \sigma_{px}^2 - \sigma_{ez}^2} \frac{2}{\sqrt{\pi}} \frac{4\pi m_e r_e^2 c^2 \eta L_c}{\gamma^3 \beta^2} . \end{aligned} \quad (4)$$

Feeding these parameters into Eq. (2) gives a prediction of the cooling rate for the case where the antiproton beam emittance is as small as it was during the drag rate measurements. For the fit shown in Figure 1 and $\delta p = 3.7$ MeV/c, Eq. (2) gives an expected cooling rate of 16 MeV/c per hour.

In operation, the transverse emittance of the antiproton beam is 5 - 10 times larger than it is during drag rate measurements. Still, Eq. (2) predicts only a slight decrease of the cooling rate because the drag force is determined primarily by electron transverse velocities. For instance, in the range of $1 < \delta p < 4$ MeV/c and $\varepsilon_n = 6\beta_f \sigma_{px}^2 / \beta \gamma c^2 < 6 \pi$ mm-mrad ($\beta_f \approx 30$ m is the average beta function in the cooling section), the calculated cooling rate given by Eq. (2) varies only by $\pm 10\%$.

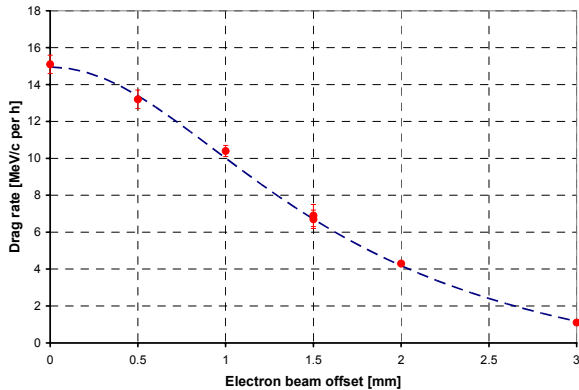


Figure 2: Drag rate as a function of the electron beam offset w.r.t. the antiprotons central orbit, for $p \equiv 3.7$ MeV/c. $I_b = 100$ mA. The dotted blue line is the fit to the data using Eq. (6) ($a = 3.72$, $b = 1.61$).

However, for large emittances, antiprotons spend a significant amount of time outside of the electron beam, which makes the model inapplicable. In addition, the drag force falls off rapidly with the offset of the electron beam with respect to the antiprotons central orbit (Figure 2).

At a typical emittance $\varepsilon_n \approx 8 \pi$ mm mrad, the rms beam radius is 2 mm, so that a significant portion of the beam is only weakly affected by electron cooling. Therefore, in the interesting range of parameters, we can ignore the weak dependence of the cooling dynamics on the antiproton transverse velocity and only take into account the radial decrease of the drag force. Furthermore, the strongest contribution to the radial dependence is expected to come from $F_0 \propto n_{eb} / \sigma_{ex}^2$,

which does not depend on the antiproton longitudinal velocity. Hence, the drag force across the beam can be interpolated as

$$F_z(\vec{V}_p, r) \approx F_{Lz}(p)_{\sigma_{px}=0} \cdot F_r(r). \quad (5)$$

We then assume that the radial dependence normalized by its maximum, $F_r(r)$, stays the same for all momenta and can be expressed as

$$F_r(r) = \left(1 - \left(\frac{r}{a} \right)^2 \right) \cdot \left(1 + \left(\frac{r}{b} \right)^2 \right)^{-1}, \quad (6)$$

where a and b are fitting parameters ($F_r(r) = 0$ for $r > a$).

In this approximation, for a Gaussian current density distribution of the antiprotons, the integral of Eq. (1) reduces to a product of its momentum and radial parts:

$$\frac{d\delta p}{dt} \approx G(p) \frac{1}{\sigma_x^2} \int_0^\infty e^{-\frac{r^2}{2\sigma_x^2}} F_r(r) \cdot r dr, \quad G(p) = \left(\frac{d\delta p}{dt} \right)_{\sigma_{px}=0}, \quad (7)$$

where σ_x is the rms size of the antiproton beam. Thus, Eq. (7), which can be computed numerically (see Fig.4), gives the longitudinal cooling rate as a function of the antiproton emittance.

COOLING RATE MEASUREMENTS

Cooling rates are measured according to the following procedure. Initially, the antiproton beam, confined by rectangular RF barriers, is cooled with the stochastic cooling system only in order to achieve antiproton momentum and transverse distributions as close as possible to Gaussian. Before the measurement starts, the bunch length is adjusted such that $\delta p \sim 3.5$ MeV/c.

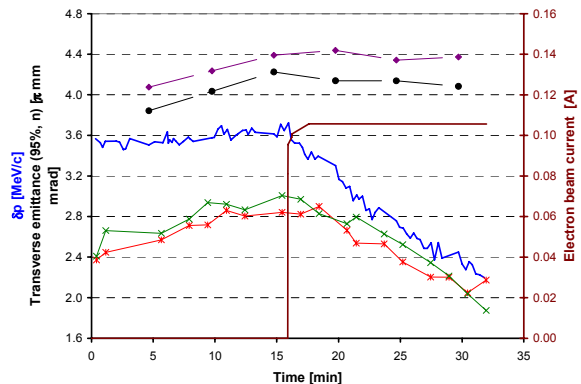


Figure 3: Evolution of δp (blue line), ε_{Sch} (red star: horizontal, green cross: vertical) and ε_{FW} (purple diamond: horizontal, black circle: vertical) during a cooling rate measurement sequence. The brown line indicates when the electron beam was turned on and set to 100 mA. $N_p = 36 \times 10^{10}$, bunch length = 5.4 μ s.

The measurement (Figure 3) consists of two parts. First, the stochastic cooling system is turned off and the antiproton beam is let diffuse for 15 minutes. Then, the electron beam is turned on, and cooling is carried on for

another 15 minutes. During the measurement, δp as well as the antiprotons 95%, normalized transverse emittances measured with a Schottky detector, ε_{Sch} , and obtained from flying wire measurements, ε_{FW} , are recorded.

The longitudinal/transverse cooling rates reported below are calculated as the difference between time derivatives of the momentum spread/emittances before and after turning on electron cooling. In the example of the measurement shown in Figure 3, the longitudinal cooling rate is found to be -7.6 ± 0.4 MeV/c per hour; the average transverse cooling rate $-5.6 \pm 0.3 \pi$ mm mrad /hr for the flying wire data and $\sim -2 \pi$ mm mrad /hr for the Schottky detector data.

Longitudinal cooling rates measured for various values of the transverse emittance of the antiprotons are shown in Figure 4, along with the curve obtained from Eq. (7) with $G(3.6 \text{ MeV/c}) = -16 \text{ MeV/c hr}^{-1}$, which relies on the data from Figure 1.

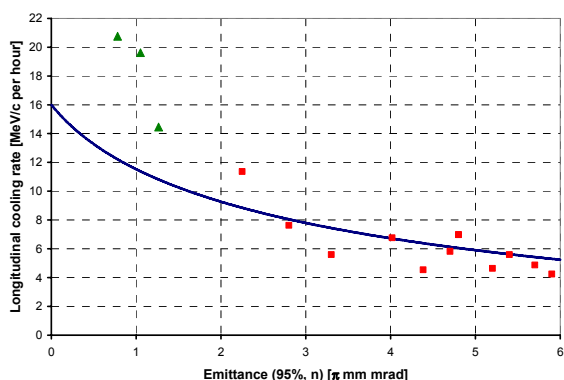


Figure 4: Longitudinal cooling rate (negated) as a function of ε_{FW} . The blue line is Eq (7) with $G(3.6 \text{ MeV/c}) = -16 \text{ MeV/c per hour}$. The electron beam was on axis for all measurements.

Note that the data points for which $\varepsilon_{FW} < 2 \pi$ mm mrad (green triangles on Figure 4) were acquired with a coasting beam that was preliminary electron-cooled. Because of a smaller δp , $0.5 - 1.6 \text{ MeV/c}$, the rate measured for these points was scaled according to Eq. (2) to the value corresponding to $\delta p = 3.6 \text{ MeV/c}$. Other points were taken at $\delta p = 3 - 4 \text{ MeV/c}$, where such scaling would not change the value by more than 4%.

The deviation of low-emittance points from the calculated curve can be attributed to several effects. In part, the numerical evaluation from Eq. (7) relies on Figure 2, which maximum amplitude is significantly smaller than the one presented in Figure 1 and the one measured concurrently with low-emittance cooling rate measurements ($15 \text{ vs } 22 \text{ vs } 30 \text{ MeV/c hr}^{-1}$). This difference is believed to result from several improvements, including a better alignment of the antiprotons with respect to the electron beam and the smoothing of the cooling section magnetic field. Most likely, it made the distribution $F_r(r)$ peakier than the one shown in Figure 2. Also, the cooling rates might be affected by the fact that the distributions recorded for the

coasting beam data points deviate from Gaussian because of the use of electron cooling at the preparation stage.

The measurements were made for a number of antiprotons $N_p = 30\text{-}200 \times 10^{10}$ particles to avoid the use of electron cooling at the preparation stage. Even a short time with the electron beam on axis changes the antiproton transverse distribution noticeably. It was found that the ratio $Re = \varepsilon_{Sch} / \varepsilon_{FW}$ can be used as a measure of the deviation of the distribution from Gaussian, because the Schottky emittance is sensitive to the tail population but the flying wire data is fitted to a Gaussian curve, effectively truncating the tails of the acquired distribution. While there is a significant unexplained discrepancy in the absolute numbers reported by these two diagnostics, their ratio is stable for near-equilibrium, stochastically-cooled distributions, $Re = 1.5 - 1.7$. For a deeply electron-cooled beam, this ratio can be as high as 5, and for the 15-min cooling measurements shown above, it takes 0.5 - 1 hour for Re to relax back to the stochastically-cooled value. As a result, typically only one such measurement was made between injections into the Recycler ($\sim 2\text{h}$).

Interpretation of the transverse emittance measurements is more difficult and their detailed analysis is still in progress.

CONCLUSION

The longitudinal electron-cooling rates are measured with an antiproton beam distribution close to Gaussian. The longitudinal cooling rate is found to significantly depend on the antiprotons transverse emittance, decreasing from its peak value by a factor of ~ 3 for emittances typical at injection, $\varepsilon_{FW} \sim 6 \pi$ mm mrad. The results compare fairly well to the trend given by a prediction that uses a semi-empirical model based on the measured dependence of the drag force on the momentum deviation and the radial offset.

ACKNOWLEDGMENTS

The authors are grateful to A. Burov and V. Lebedev for fructuous discussions regarding the theoretical aspects of the paper. We also would like to thank M. Hu and D. Broemmelsiek for their efforts with the beam diagnostics. Discussions with A. Fedotov and A. Sidorin and their participation in a set of measurements are appreciated.

REFERENCES

- [1] A. Shemyakin *et al.*, Proc. of EPAC'06, Edinburgh, UK, June 26-30, 2006, TUPLS069, 1654-1656.
- [2] Ya.S. Derbenev and A.N. Skrinsky, Particle Accelerators **8** (1977) 1.
- [3] I.N. Meshkov *et al.*, Physics guide of BETACOO code, v.1.1, BNL note C-A/AP#262, p. 17.
- [4] A. Shemyakin, FERMILAB-TM-2374-AD.
- [5] L. Prost *et al.*, in Proc. of HB2006, Tsukuba, Japan, May 29-June 2, 2006, WEAY02, p 182.